THE ROLE OF CAPILLARY FORCES IN THE NATURAL STATE OF FRACTURED GEOTHERMAL RESERVOIRS

N. Noel. A. Urmeneta, Shaun Fitzgerald and Roland. N. Home

Stanford Geothermal Program, Dept. of Petroleum Engineering., Stanford University, CA 94305-2220, USA

Abstract

A lot of experiments into the natural state of geothermal reservoirs have been conducted using porous medium models, even though geothermal systems are usually highly fractured. It is unclear whether a porous medium model is adequate in describing the natural state of a fractured geothermal reservoir. Because of this, a dual porosity model is often invoked. The question of how heat and mass is transferred in fractures has been widely investigated. The objective of this work was to further our understanding by investigating how heat and mass transfer is affected by capillaty forces. Also, the question of how capillary forces affect the stability of a water-saturated region overlying a liquid-dominated two-phase zone was examined. The study was carried out by developing a two-dimensional numerical model representing a fractured geothermal reservoir. The numerical simulations were carried to steady state with the use of a commercial simulator TETRAD (version 12). Results indicate that due to capillaty forces, the fractures act as heat pipes - transporting heat by the process of convection. The convection process was found to be enhanced if there is no capillaty pressure in the fractures. It was also determined that only if capillary forces are present can a system consist of a water-saturated zone overlying a liquid-dominated two-phase zone remain stable.

1. INTRODUCTION

Much of the experimental work which pertains to geothermal systems has involved studies on porous media. Although most geothermal reservoirs are observed to be fracture dominated, experimental results involving porous media are often still applied. It is unclear whether a porous medium model is adequate in describing a fractured geothermal reservoir since there are some situations where the fractured nature of the reservoir cannot be ignored. One case involves the injection of cold brine (normally around 160°C) as a means of pressure support or for environmental reasons. If the geothermal system were to behave like a homogeneous porous medium, the thermal front would advance uniformly with the cooler fluid sweeping away the heat from the rock. In reality, this will not be the case. There will be a preferential flow through the fractures and even though there is transfer of heat by conduction from the rock to the cold water passing through the fractures, the injected water will arrive much sooner than in the case of a porous medium. Because of this problem, a dual porosity mode! is often invoked. Instead of treating the reservoir as homogeneous, fractures are introduced by dividing the system into two types of interacting porous media as can be seen in Fig. 1. The matrix is assigned a permeability, k_m, and a porosity, ϕ_m, while the fracture is assigned a higher permeability, k_f, and a higher porosity, ϕ_f.

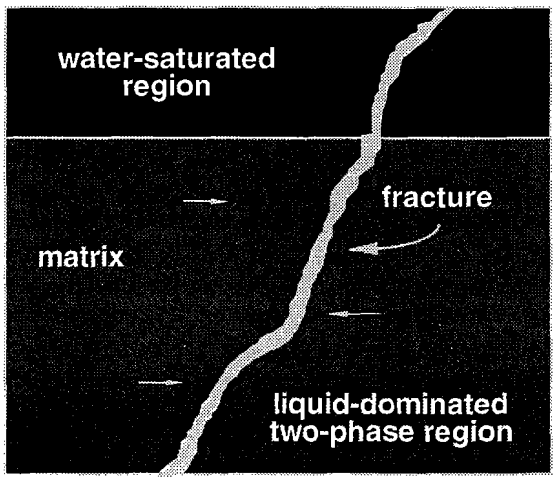

Fig. 1. A dual porosity model.

In a dual porosity model, the question of how heat is being transferred from the rock matrix to the fluid flowing in the fractures has been investigated. Previous works include those by Bodvarsson (1969, 1972), Drummond and McNabb (1972) and Nathenson (1975). The objective of this work was to further our understanding by investigating how heat and mass transfer is affected by capillary forces. To address this issue, it is worthwhile to investigate the heat pipe effect. The heat pipe mechanism (Eastman, 1968) allows the upward movement of heat in a system that exhibits a very small temperature gradient. Since this problem is reasonably understood from earlier work, looking into the heat pipe mechanism would enable us to understand the effect of capillary pressure on the behavior of fractured reservoirs.

White et al. (1971) proposed a conceptual model of a vapor-dominated geothermal reservoir. The model has a deep-seated convecting brine which is heated by a magmatic heat source. On top of this convecting brine is a two-phase region whose vapor and liquid phases undergo counterflow convection. This two-phase region is separated from the overlying zone of meteoric water and steam condensate by a caprock. For liquid-dominated systems, most of the conceptual models likewise invoke the presence of a caprock. Such is the case for the Tongonan geothermal reservoir in the Philippines (Grant and Studt, 1981) and the Wairakei geothermal field in New Zealand (Grindley, 1965).

Sondergeld and Turcotte (1977) did experimental studies on two-phase thermal convection in a porous medium. They were able to observe that a counterflowing two-phase zone can be stable beneath a water-saturated zone (Fig. 1). This experimental result suggests that geothermal reservoirs need not have to have a caprock. How is this possible? Will the presence of fractures destabilize the arrangements of fluids? What will be the influence of capillarity in permitting this configuration? One of the objectives of this study was to explore the stability of a water-saturated zone overlying a two-phase zone. The investigation on the stability of such systems was limited, however, to the case of a liquid-dominated two-phase reservoir.

To answer these questions, a numerical investigation was conducted utilizing the commercial program TETRAD (version 12). The approach utilized in this study involved the concept of building complexity. To start with, a one-dimensional numerical model was built in order to examine the heat pipe effect. This model was then extended to two dimensions. With this model the effect of capillary forces on heat and mass transfer as well as on stability was investigated by varying the capillary pressure curves.

2. PRELIMINARY WORK

Prior to the development of the two-dimensional numerical model used in this study, a one-dimensional numerical model was constructed in order to duplicate some of the results obtained by previous investigators who worked on heat pipes. Having a one-dimensional numerical model that conforms with experimental and theoretical results reinforces the validity of the model. Being confident with the one-dimensional model, the two-dimensional model was constructed in a similar fashion to the one-dimensional case. Since the numerical model now had two dimensions, the question of which differencing scheme, whether a five-point differencing scheme or a nine-point differencing scheme, is appropriate for the numerical model was raised. Likewise, the type of capillary pressure functions to be used in the study had to be determined.

2.1 One-dimensional model

The one-dimensional model consisted of a 7 m x 50 m x 1 m block and ten 7 m x 50 m x 50 m blocks stacked on top of each other as shown in Fig. 2. The model represents a homogeneous system and the properties assigned to each block are summarized in Table I. The topmost block was given a very large volume in order to impose a constant pressure and saturation condition at the top. The blocks were initially saturated with water. With a 1 W/m^2 heat flux imposed at the bottom block, numerical simulation was carried out until steady state conditions were attained.

Table I. Parameters of the one-dimensional model.

Property	Block 1 (Large volume element)	Blocks 2 - 11 (Matrix blocks)
Porosity	0.8	0.1
Permeability (md)	2000	0.5
Rock density (kg/m^3)	2643	**2643**
Rock conductivity (W/m-°C)	2.88	2.88
Rack specific heat (kJ/kg-°C)	1.0718	1.0718
Heat flux (W/m^2) - block 11		1.0
Relative permeability	$k_{rl} = (S)^3$ $k_{rv} = (1-S)^3$	$k_{rl} = (S)^3$ $k_{rv} = (1-S)^3$

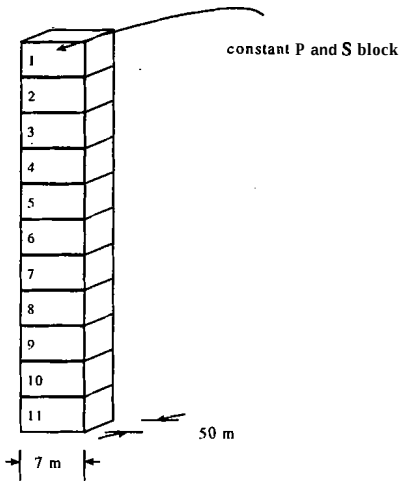

Fig. 2. One-dimensional model **of** a heat pipe.

Results indicated that two-phase conditions were present at a depth of 175 m (block no. **5)** down to the bottom. In this two-phase region vapor rises up to block no. 5 while liquid trickles from block no. 5 down to the bottom. There was a counterflow of the liquid and the vapor phases within the two-phase zone. **A** plot of the dimensionless heat flux versus saturation is shown in Fig. **3.** The analytical solution and the dimensionless heat flux for each block was derived for the cubic relative permeability curves (Table I) utilizing the same procedure Bau and Torrance (1982) used. The dimensionless heat fluxes for each block were calculated using the following equation:

$$\Gamma = \frac{q\nu_v}{\lambda h_{lv} g(\rho_l - \rho_v)} = \frac{S^3(1-S)^3}{(1-S)^3 \frac{\nu_l}{\nu_v} + S^3} \quad (1)$$

where

Γ = dimensionless heat flux
q = vertical heat flux
ν_v = vapor kinematic viscosity
ν_l = liquid kinematic viscosity
h_{lv} = latent heat of vaporization
λ = permeability
ρ_l = liquid density
ρ_v = vapor density
g = acceleration due to gravity
S = liquid saturation

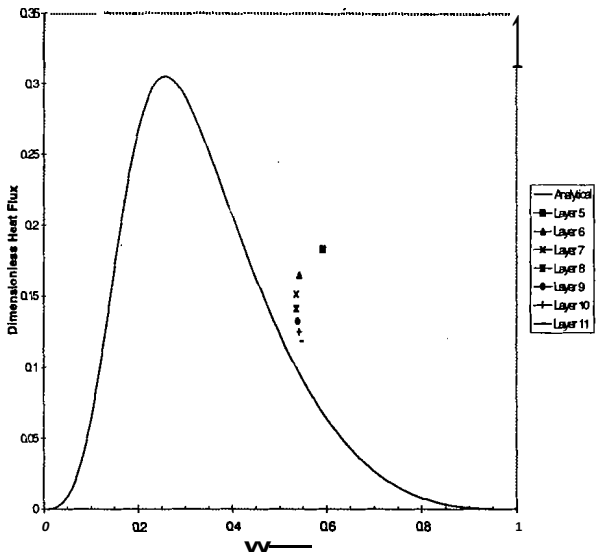

Figure 3. Plot **of** the dimensionless heat flux versus saturation for a cubic relative permeability curve.

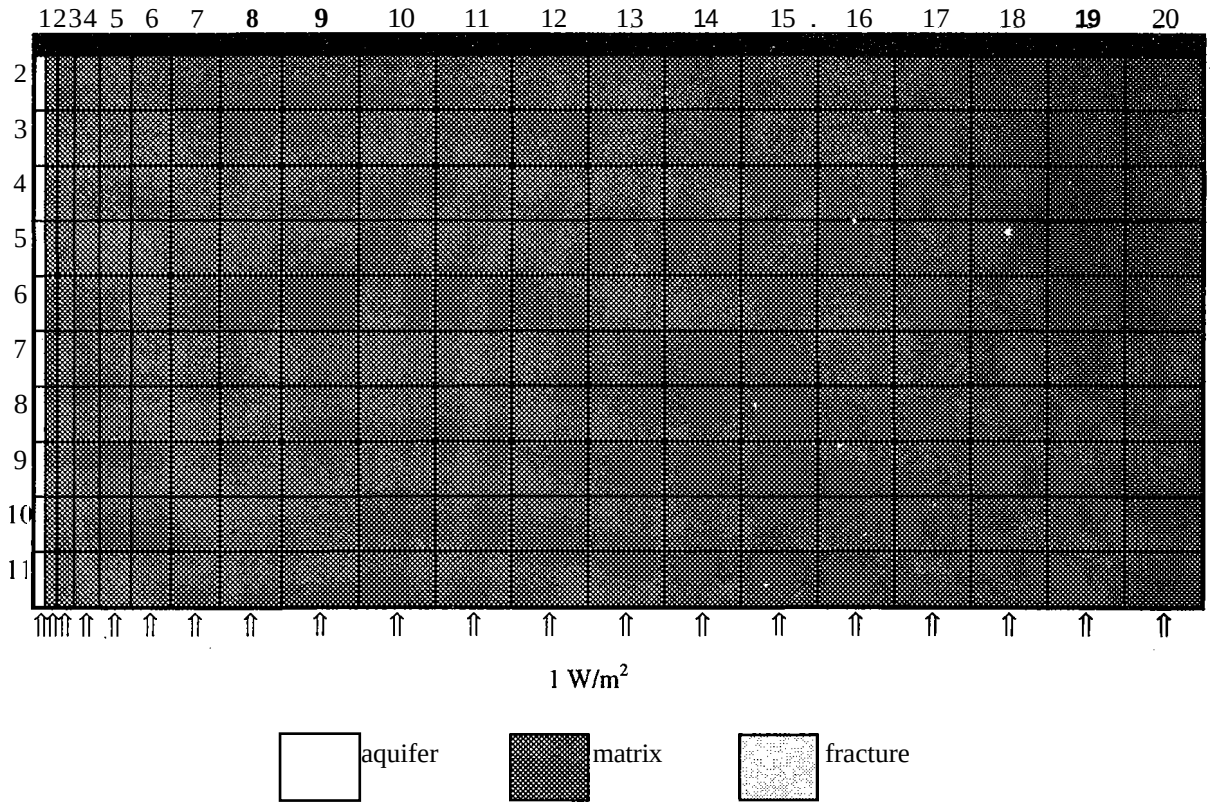

Fig. 4. The 20 x 11 x 1 block model.

The points do not plot on the line representing the analytical solution but instead lie to the right of it. One possible explanation is that the heat transfer mechanism in this one-dimensional system involves both convection and conduction, whereas the analytical solution does not take conduction into account. The graph however shows that we were able to produce a liquid-dominated heat pipe since the water saturations were above the saturation corresponding to the maximum heat flux, in this case, 0.26.

2.2 Two-dimensional model

With the existing one-dimensional model, a two-dimensional grid was produced by having 20 grid blocks in the x direction instead of just having one and maintaining the number of layers in the z direction. The grid system is shown in Fig. 4. The model had dimensions of 7 m x 501 m x 50 m and consisted of 220 blocks. The first two columns had a length of 0.01 m, the third column had a length that is twice that of the previous one and this progression continued until the seventh column had a length of 0.32 m. The eighth column had a length of 0.36 and the remaining 12 columns had a length of 0.5 m. The depth and width of each grid block was 50 m. The blocks in the first layer were assigned very large volumes and were fully saturated with water hence these large volume blocks were termed the aquifer blocks. The rest of the blocks were labeled as matrix blocks. The same properties outlined in Table I were assigned to this two-dimensional numerical model. The same heat flux of 1 W/m^2 was delivered to the blocks at the bottom layer.

To achieve steady state, the model was ran up to a time of 4 x 10^6 days. The results showed no variation in the temperature, pressure and saturation values along the x direction in all the layers. Even though a two-dimensional grid was used, the system behaved like the one-dimensional case due to the fact that the system was homogeneous. Likewise, the graph of the non-dimensional heat flux as a function of water saturation looks exactly like Fig. 3. With this two-dimensional model, the stability of a water-dominated region over a liquid-dominated two-phase system was demonstrated.

The fact that the two-dimensional model with uniform matrix properties was able to duplicate the behavior of the one-dimensional model reinforces the validity of both models as well as that of the

simulator itself. After having shown that a water-dominated region can be stable over **a** liquid-dominated two phase region, the next question was, how would this stability be affected by the presence of fractures.

The reason why the grid was designed as in Fig. 4 was in order to model a fracture on the left-hand side. Hornbrook and Faulder (1993) modeled a fracture by having large-blocks (10 m wide) which were assigned a porosity of 0.0001 in order to simulate a 1 mm fracture. The fracture in this case was modeled by having blocks which were thin (0.01 m wide) and which were given a porosity of 0.5 in order to simulate a 0.005 m fracture. By specifying a larger permeability and porosity to the blocks in column 1 as compared to the matrix blocks (Fig. 4), a fracture at the left-hand side of the model was created. This two-dimensional model with both fracture and matrix blocks was the one used in the investigation.

2.2.1 Five-point versus nine-point differencing schemes

The standard approach in numerical simulation work is to make use of the five-point differencing scheme in the discretization of the differential equations describing reservoir flow. In a two-dimensional grid, the flow in and out of a computational grid point is influenced by the points directly to the sides, above and below it. With a higher order differencing scheme, such as a nine-point, the four computational grid points along the diagonals are also taken into account. Pruess (1991) indicated that although there are cases where the five-point differencing scheme is appropriate, there are certain situations where the nine-point differencing scheme is better. Pruess showed that a higher-order differencing scheme substantially diminishes the grid orientation effects. The study done by Hornbrook and Faulder (1993) asserted that the nine-point differencing scheme was more appropriate. The question then was, which differencing scheme is appropriate for the two-dimensional system in this study?

To address this issue, we made use of a 5 x 1 x 11 block numerical model whose properties were similar to the model described in Section 3.2. The dimensions, however, were 25 m x 50 m x 501 m. Using the five-point differencing scheme, the steady state solution was simulated. Three other simulation runs utilizing the five-point differencing scheme were performed using different models. The second model had 10 blocks in the **x** direction while the third and fourth ones had **14** and 18 blocks, respectively. The numerical runs indicated that with the five-point differencing scheme, the results obtained were consistent. The steady state solution was independent of the grid system used.

A second set of simulation runs was conducted using the same set **of** models. However, this time the nine-point differencing scheme was utilized. Results indicated that the steady state solution for each run was dependent on the grid system used.

A comparison between experimental and numerical results was done in order to further examine the applicability of the five-point differencing scheme. The experimental results obtained by Bau and Torrance (1982) for a porous bed with permeability of 8.5 d were simulated using a radial grid model. The centerline temperatures obtained from experiments were compared to those obtained from the numerical model where a five-point differencing scheme was used. Fig. 5 shows that the numerical results replicate the experimental results especially in the two-phase regions.

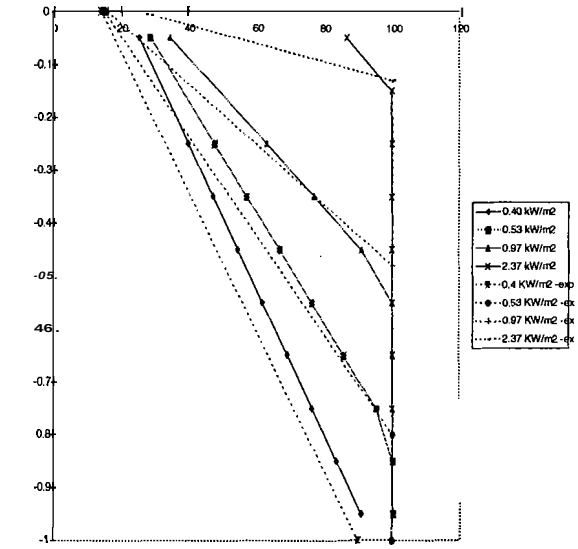

Fig. 5. A comparison between the centerline temperatures obtained from Bau and Torrance's (1982) experiment and the radial grid numerical model.

From these observations, we determined that the five-point differencing scheme was more appropriate than the nine-point differencing scheme for this type of problem. Hence, all the subsequent

numerical runs used the five-point differencing scheme.

2.2.2 Capillary pressures

The two-dimensional model described earlier has three different domains - the aquifer, the matrix and the fracture blocks. A primary issue in the study was to determine the appropriate capillary pressure functions for the different domains.

For the aquifer blocks, since we wanted all of the liquid to be mobile we imposed zero capillary pressure. For the matrix blocks, the capillary pressure curves were similar to those derived from a typical Geysers isotherm (Satik et al., 1996), as described by the van Genuchten equation:

$$p_c = p_o\left(S_{ef}^{-1/\lambda} - 1\right)^{1-\lambda} \qquad (2)$$

where p_o and λ are constants. S_{ef} is the effective liquid saturation given by

$$S_{ef} = \frac{S - S_r}{1 - s_r} \qquad (3)$$

where S_r is the residual water saturation (Pruess et al., 1992). For the fracture blocks, we first thought that since the fracture has a large equivalent pore size, the capillary pressure would approach zero and hence would be independent of the saturation. Simulation runs were carried out using constant capillary pressures that ranged from 0 to 200 kPa for the fracture blocks. The simulation runs did not converge to a steady state solution. Hence, a linear capillary pressure function was used instead. A linear capillary pressure function was also utilized by Pruess (1985) and Hornbrook and Faulder (1993) for the fracture blocks in their studies.

3. THE EFFECT OF CAPILLARITY ON STABILITY AND FLUID FLOW BETWEEN THE FRACTURE AND THE MATRIX

It has been established in Section 2.2 that a water-saturated zone can remain stable over a liquid-dominated two-phase region. The question is, what would happen to this stability when a fracture is added to the system. Will the system become unstable and flip over? What role do capillary forces have on the observed stability? If the system is in fact stable even with the presence of the fracture, how do capillary forces affect the heat and mass transfer between the fracture and the matrix? These issues will be discussed in this section.

3.1 The two-dimensional models

The two-dimensional model constructed in Section 2.2 was utilized. The matrix and fracture properties are summarized in Table II. There were five models used in this study, each differing in the type of capillary pressure function imposed on the fracture blocks.

Table 11. Parameters of the two-dimensional model used in the simulation.

Property	Aquifer	Matrix	Fracture
Porosity	0.8	0.1	0.5
Permeability (md)	2000.0	0.5	50.0
Rock density (kg/m^3)	2643	2643	2643
Rock conductivity (W/m-°C)	2.88	2.88	2.88
Rock specific heat (kJ/kg-°C)	1.0718	1.0718	1.0718
Heat flux (W/m^2) - blocks 201-220		1.0	1.0
Relative permeability	$k_{rl} = (S)^3$ $k_{rv} = (1\text{-}S)^3$	$k_{rl} = (S)^3$ $k_{rv} = (1\text{-}S)^3$	$k_{rl} = (S)^3$ $k_{rv} = (1\text{-}S)^3$

Table III. The capillary pressures used for the different models.

Model	Aquifer	Matrix	Fracture
	0	$p_{cm} = 0$	$p_{cf} = 0$
	0	$p_{cm} = 100\left(S^{-1/0.6} - 1\right)^{0.4}$	$p_{cf} = -200S + 200$
	0	$p_{cm} = 100\left(S^{-1/0.6} - 1\right)^{0.4}$	$p_{cf} = -100s + 100$
	0	$p_{cm} = 100\left(S^{-1/0.6} - 1\right)^{0.4}$	$p_{cf} = -50S + 50$
	0	$p_{cm} = 100\left(S^{-1/0.6} - 1\right)^{0.4}$	$p_{cf} = 0$

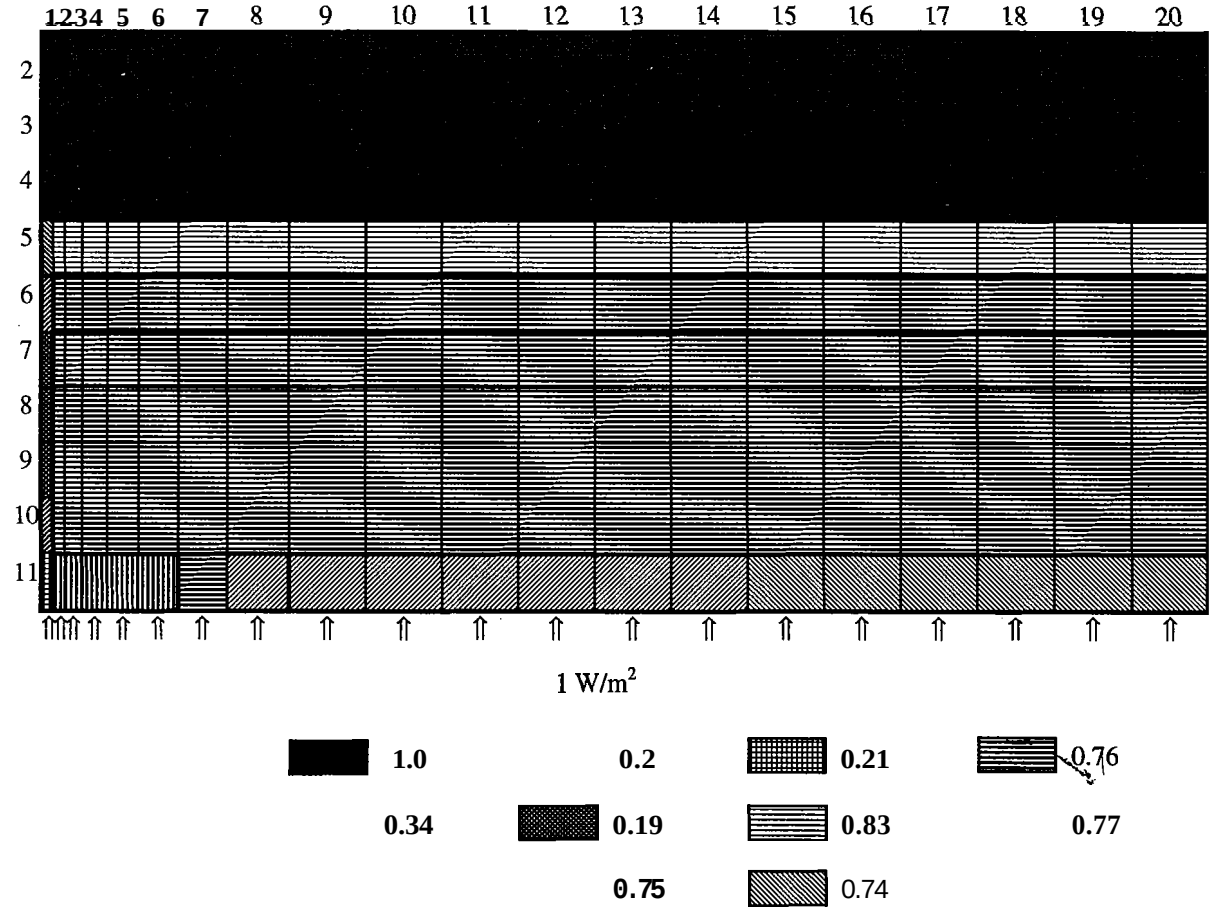

Fig. 6. Liquid saturation distribution for Model 111.

The matrix capillary pressure is described by the equation

$$p_c = 100\left(S^{-1/0.6} - 1\right)^{0.4} \quad (4)$$

while the fracture capillary pressure is described by the equation

$$p_{cf} = -A(S) + A \quad (5)$$

where S is the water saturation and A is the maximum-fracture capillary pressure in kPa. There was no capillary pressure function assigned to the aquifer blocks. The capillary pressure functions used in the different models are shown in Table 111.

Using TETRAD version 12, simulations were carried out for up to 4×10^6 days in order to reach steady state.

3.2 Results and discussion

For Model I where no capillary pressures were prescribed, the two-phase region underneath the water-saturated zone collapsed. The temperature, pressure and saturation profiles indicate that we have a water-saturated region occupying the entire system.

For Model II where a van Genuchten type of capillary pressure curve was prescribed for the matrix blocks and a linear capillary pressure curve with a maximum value of 200 kPa was prescribed for the fracture blocks, an oscillatory behavior was observed for the temperature, pressure and saturation profiles with time. The period of oscillation was 3.5 cycles per 1×10^5 days.

For Model III where the maximum capillary pressure in the fracture blocks is 100 kPa, a water-saturated region remains stable on top of the two-phase zone. The saturation distribution is shown in Fig. 6. It was not unlikely that the fracture blocks, being highly permeable, would easily become saturated with water from the overlying four layers of fully water-saturated rock matrix. The numerical results obtained, however, indicate otherwise. In fact, the fracture has an average steam saturation of 80% while the adjacent matrix blocks are on the average 75% saturated with water.

The dimensionless heat flux for the fracture blocks in the two-phase region were calculated using Equation 1. These points when plotted versus saturation would lie towards the vapor-dominated heat pipe solution (Fig. 7). It can be noted that the point from Layer 5 is far from the analytical curve. This point actually belongs to the block that serves as an interface between the water-saturated and the vapor-dominated regions. Figure 7 indicates that the fracture blocks in Layers 6 to 11 form a vapor-dominated heat pipe.

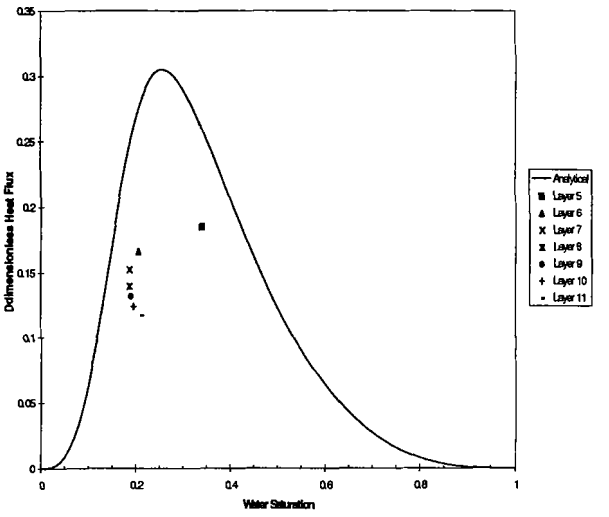

Fig. 7. Plot of the dimensionless heat flux versus saturation for the fracture blocks of Model 111.

For Model IV, the maximum capillary pressure in the fracture blocks was decreased by 50 kPa. The saturation field is shown in Fig. 8. When the maximum capillary pressure in the fracture blocks was decreased to 50 kPa, the amount of water retained in the fracture blocks decreased. The average steam saturation in the fracture blocks within the two-phase zone was 85%. Correspondingly, the amount of fluid in the matrix blocks increased. The average water saturation in the matrix blocks became 93%. Calculations for the heat flux within the fracture blocks would indicate that we do have a vapor-dominated heat pipe (Fig. 9). The points are much nearer to the line representing the analytical solution.

The results from Model V show that the matrix blocks are almost entirely water-saturated (Fig. 11). Examination of the pressure, temperature and saturation distribution within the fracture blocks and the plot of the dimensionless flux versus saturation (Fig. 10) indicates that the fracture is actually a vapor-dominated heat pipe. When compared to Model IV, the saturations are not significantly different.

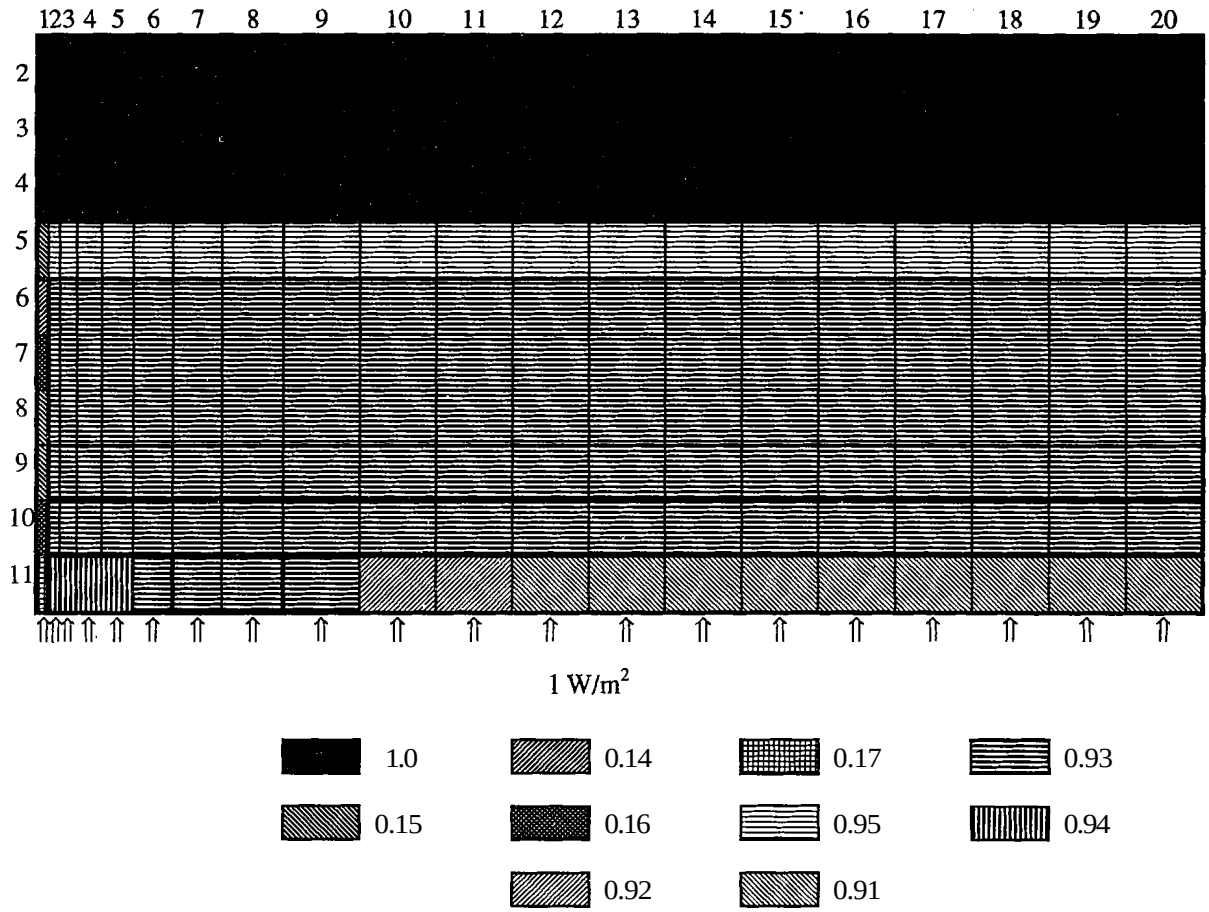

Fig. 8. Liquid saturation distribution for Model IV.

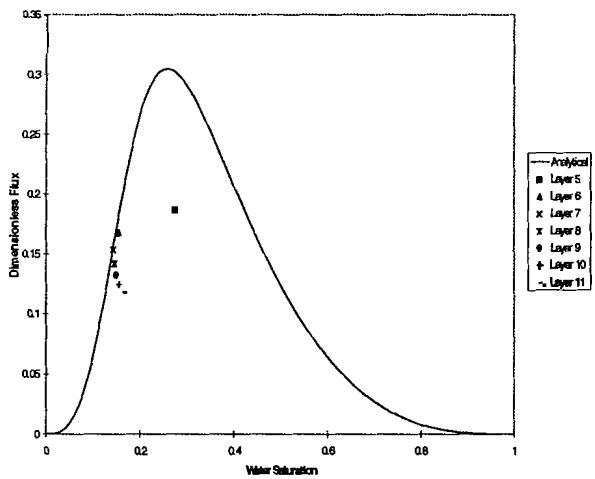

Fig. 9. Plot of the dimensionless heat flux versus saturation for the fracture blocks of Model IV.

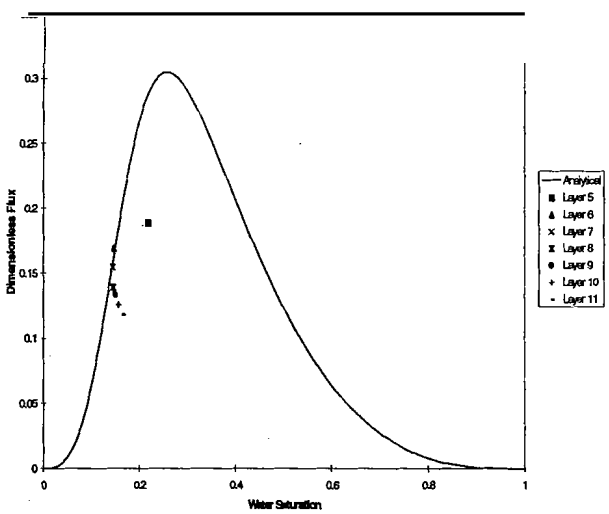

Fig. 10. Plot of the dimensionless heat flux versus saturation for the fracture blocks of Model V.

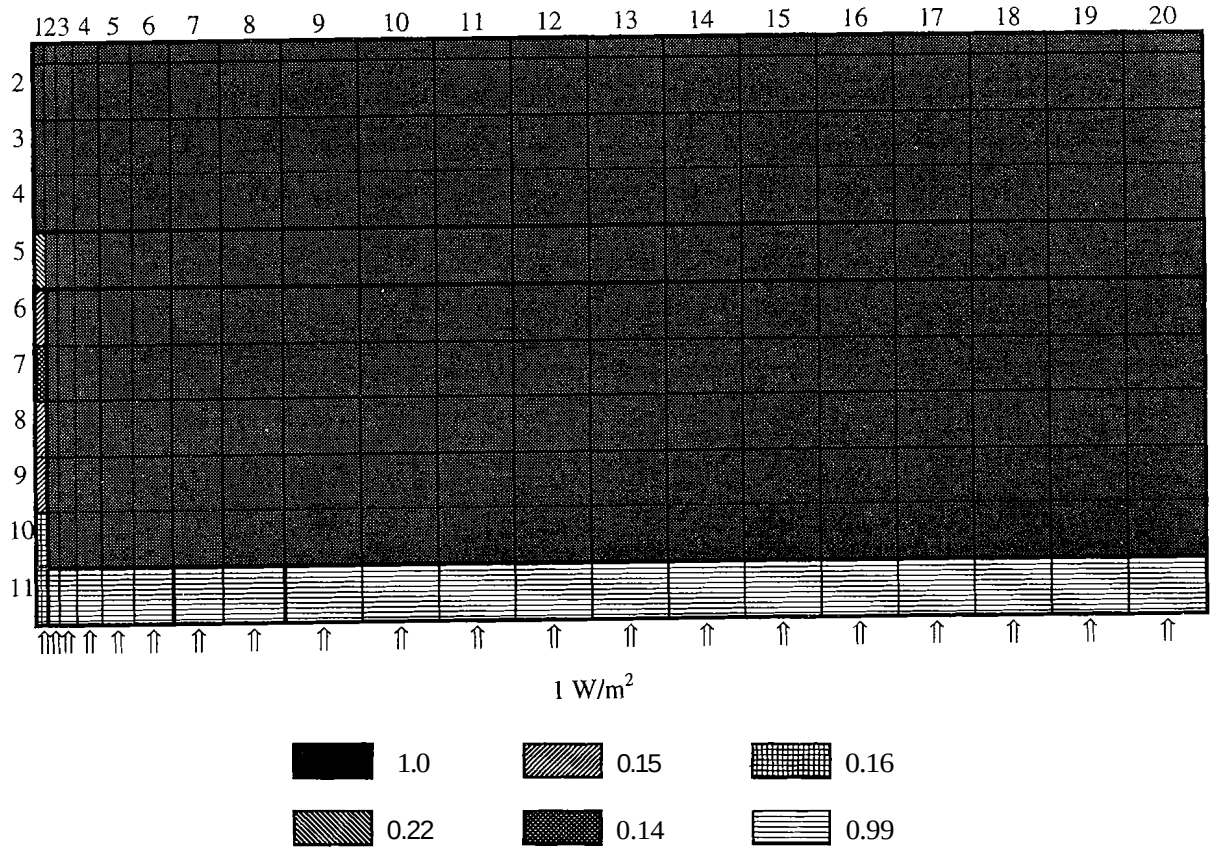

Fig. 11. Liquid saturation distribution for Model V.

On the issue of stability, Model I indicates that numerically it is not possible to maintain a water-saturated region on top of a liquid-dominated two-phase fractured reservoir if no capillary pressure functions are specified for both the matrix and the fracture blocks. However, Model V gave the result that even if no capillary pressures were specified for the fracture blocks, a small two-phase zone could still exist below a water-saturated zone. Combining these observations, we can say that not specifying capillary pressures in the matrix blocks would destroy the stability of water over a liquid-dominated two-phase region.

From Models III to **V,** it can be observed that the fracture acted like a heat pipe and as the maximum capillary pressure specified on the fracture blocks is diminished, the average steam saturation increases. This is due to the fact that capillary forces tend to suck the liquid phase into the pores of the porous medium. In the presence of vapor, the capillary forces through adsorption would induce capillary condensation and the net effect is to have a higher liquid saturation. Not specifying capillary pressures in the fracture increases the heat pipe effect. This is good if we want to **look** at it in terms of heat transfer. Heat is transmitted more effectively since the mode of heat transfer is through convection. Steam rises through the fractures and on reaching the water-saturated region, loses energy, condenses and trickles down. Liquid is also transferred from the matrix blocks into the fracture where it boils off and rises as steam. Numerical results indicate that as the capillary pressure in the fracture is diminished, the rate at which liquid is transferred from the matrix into the fracture is increased. Likewise, the steam flux going through the fracture is increased. In other words, convection is enhanced and so is heat transfer.

4. CONCLUSIONS

Capillary forces play an important role in determining the natural state of fractured geothermal reservoirs. Capillarity tends to keep the vapor phase in the fractures and the liquid phase in

the matrix. In this manner, the fractures are not fully saturated with liquid and the possibility of having a heat pipe is increased. In Models III to V, the fractures were actually vapor-dominated heat pipes. Not having capillary pressure in the fracture blocks enhances the heat pipe effect, and also increases the transfer of liquid from the matrix into the fracture. Having low or no capillary pressure specified in the fracture blocks would improve the convection process and hence speed up heat transfer.

Based on the results obtained from Model II, it seems that the appropriate value for capillary pressures in fractures should not reach 200 kPa. This is reasonable due to the inverse relationship capillary pressure has with the mean pore radius. Since the mean pore radius is "large," small capillary pressures are expected.

Capillary pressures are likewise important as far as the stability of a water-saturated region on top of a liquid-dominated two-phase zone is concerned. Not specifying a matrix capillary pressure (Model I) will cause the two-phase zone to collapse under the water-saturated zone.

The two-dimensional fractured model demonstrates that due to capillary forces, a liquid-dominated two-phase zone will remain stable under a water-saturated region. Normally, one would think that due to the presence of a high permeability conduit, the liquid would gush through the fracture and quench the two-phase zone, however, this is not necessarily the case.

The numerical stability of this system suggests that it is not necessary to model a geothermal system as having a caprock on top. This is the same observation made by Sondergeld and Turcotte (1977) based on their experimental results.

ACKNOWLEDGEMENT

This work was funded by the U.S. Department of Energy under grant number DE-FG07-95ID13370.

REFERENCES

Bau, H. M. and Torrance, K. E. (1982). Boiling in low-permeability porous materials. *Int.* J. of *Heat Mass Transfer* **25**, 45-55.

Bodvarsson, G. (1969). On the temperature of water flowing through fractures. J. *Geophys. Res.* 74(8), 1987-1992.

Bodvarsson, G. (1972). Thermal problems in the siting of reinjection wells. *Geothermics* 2(1), 63-66.

Drummond, J. E. and McNabb, A. (1972). The heating of cold-water intrusions in a geothermal field. *N.* Z. J. *Sci.* 15(4), 665-672.

Eastman, G. Y. (1968): The heat pipe. *Sci. American* 218, 38-64.

Grant, M. A. and Studt, F. E. (1981). A conceptual model of the Tongonan geothermal reservoir. ***Pap. GEOSEA** Conf. 4th, 1981.*

Grindley, G. W. (1965). Wairakei. ***New Zealand Volcanology.*** 157.

Hornbrook, J. W. and Faulder, D. D. (1993). Parametric analysis of factors affecting injection and production in geothermal reservoirs. ***Proc. Stanford Geoth. Workshop*** 18, 53-60.

Nathenson, M. (1975). Physical factors determining the fraction of stored energy recoverable from hydrothermal convection systems and conduction dominated areas. ***Geol. Surv. Open-File Rep.*** (U.S.) 75-525.

Pruess, K. (1985). A quantitative model of vapor dominated geothermal reservoirs as heat pipes in fractured porous rock. ***Geothermal Resources Council: Transactions*** 9(II), 353-361.

Pruess, K. (1991). Grid orientation and capillary pressure effects on the simulation of water injection into depleted vapor zones, ***Geothermics*** 20(No.5/6), 257-277.

Pruess, K. and O'Sullivan M. (1992). The effects of capillarity and vapor adsorption in the depletion of vapor-dominated reservoirs. ***Proc. Stanford Geoth. Workshop*** 17.

Satik, C., Walters, M. and Horne, R. N. (1996). Adsorption characteristics of rocks from the vapor-dominated reservoir at the Geysers, CA. ***Proc. Stanford Geoth. Workshop*** 21,469-479.

Sondergeld, C. H. and Turcotte, D. L. (1977). An experimental study of two-phase convection in porous medium with applications to geological problems. J. ***Geophys. Res.*** 82(14), 2045-2053.

White, D. E. L., Muffler, J. P. and Truesdell, A. H. (1971). Vapor-dominated hydrothermal systems compared with hot-water systems. ***Econ. Ceol.*** 66,75-97.